# Chapter 8

# The Galactic Distribution of Large H I Shells

**Abstract**

We examine the distribution of large H I shells in the Milky Way. Several of the shells are located between the spiral arms of the Galaxy. We explore possible explanations. In particular, we explore whether the density gradient away from spiral arms, combined with the many generations of sequential star formation required to create large shells, could preferentially place shells on the trailing edges of spiral arms. Spiral density wave theory is used in order to derive the magnitude of the density gradient behind spiral arms and compare this with the gradient out of the plane. We find that the density gradient away from spiral arms is comparable to that out of the Galactic plane and therefore suggest that this may lead to exaggerated expansion away from spiral arms and into the interarm region.

## 8.1 Introduction

H I shells are expected to be correlated with massive star formation, which is highest in the arms of a spiral galaxy. Though the direct correlation between large H I shells and OB associations is not always apparent, it is nonetheless expected that H I shells will form where there are stars and therefore should be located in spiral arms. This, however, is not always true. The largest shells, such as those presented in Chapter 5, may require as many as 1000 massive stars to reach their present sizes and rates of expansion. A typical OB association is likely to have only 20-40 stars (Humphreys 1978). Therefore, in order for a shell to reach a size of several hundred parsecs, it must have been associated with many sequential cycles of star formation. Our understanding of spiral structure suggests that the required generations of stars are much more likely to occur within a spiral arm as the spiral density wave passes through the gas and triggers star formation. The many cycles of sequential star formation required to create large shells, therefore, may contribute to a spatial offset of shells away from the shock at an arm's leading edge.

Nineteen new large H I shells were presented in Chapter 5. When discussing the properties of these shells we also included H I shells from Heiles (1984, 1979). Here we discuss these shells with regard to their Galactic distribution. We address the question of why so many large H I shells are found in the outer regions of galaxies and we relate the spatial distribution to spiral structure. The spatial distribution of H I shells in a spiral galaxy has been examined by several authors (e.g. Ehlerová & Palouš 1996; Thilker 1999). In an attempt to explain H I shell energetics, Ehlerová & Palouš (1996) examined the distribution of H I shells in the Milky Way. In particular, they sought evidence, through the distribution, for a high velocity cloud (HVC) formation mechanism. They concluded that because the radial distribution of shells in the Galactic plane is similar to the distribution of stars there is no evidence for prevailing a HVC formation mechanism. Thilker (1999) briefly discussed the distribution of H I shells in

NGC 300, NGC 2403, M81, and M101. His study focused on a differentiation between shell properties (i.e. radius and expansion velocity) for distinct regions in the galaxy disks. The present study differs from these studies in its attempt to put the spatial distribution of H I shells in the context of spiral structure.

In order to explain an excessively large formation energy for GSH 277+0+36, implied by its large radius ($R_{sh} \approx 220$ pc) and rapid expansion ($v_{exp} \sim 20$ km s$^{-1}$), we suggested that shells formed on the edge of spiral arms may experience exaggerated expansion into the interarm region, much as they do away from the plane (§ 3.4). In this case, we suggested that the pressure gradient on the trailing edges of spiral arms may cause shells to expand away from the gravitational potential well of the arm and into the less dense interarm region. We raised this point again in Chapter 4 with regard to GSH 304-00-12. We might expect, then, to find the largest supershells on the trailing edges of spiral arms. One result of exaggerated expansion is a falsely high calculated expansion energy. If the average formation energy requirements were reduced it could help to settle concerns about large shell formation energies in the outer regions of galaxies. In this chapter we explore these suggestions.

In section 8.2 we examine the spatial distribution of H I shells in the Milky Way. In section 8.3.1 we develop the basics of spiral structure which we apply to explain the spatial distribution of shells. We examine the density gradient on the back side of spiral arms and compare this with the density gradient away from the galactic disk. In conclusion, although there is no apparent global trend in the spatial distribution of H I shells in the Milky Way, there are many large shells in interarm regions and we offer an explanation as to why.

## 8.2 Spatial Distribution of H I Shells

We first examine an azimuthally averaged sample of H I shell size versus Galactic radius. It has long been noticed in external galaxies, as well as in the Milky Way, that the largest H I shells tend to be located at large galactocentric radii (e.g. Heiles 1979; Deul & den Hartog 1990; Walter & Brinks 1999; Crosthwaite et al. 2000). Walter & Brinks (1999) noted that in other galaxies, where the distance ambiguities that plague distribution studies of the Milky Way are non-existent, most large shells are at galactocentric radii of more than 50% of the exponential scale length. Furthermore, two-dimensional hydrodynamical simulations by Wada & Norman (1999) show that larger H I cavities are created at outer radii than at inner radii. They attribute this to the disruptive effects of supernovae on the creation of large-scale structures. Fig. 8.1 shows the radius of SGPS and Heiles (1979, 1984) shells as a function of galactocentric radius. Clearly, the largest shells are also at large Galactic radii. As mentioned in § 5.2.1, the reader should beware that Galactic H I shell catalogs exhibit a bias towards outer Galaxy shells. However, the identification of the same trend in external galaxies leads us to believe that it is real.

The number of large shells outside of the solar circle offers a challenge to the theory of shell formation from stellar winds and supernovae. Given that several hundred stars are needed to create shells with radii of a few hundred parsecs it is difficult to understand how the star formation rates in the outer Galaxy can be high enough to sustain so many large shells. Although the star formation rates initially seem unreasonable, the relationship of the shell size to the ambient density into which the shells expand should be considered. If the ambient densities are lower in the outer Galaxy, as was found around several shells in our catalog, then shells there can reach larger sizes than those in the inner Galaxy. However, this is not a strong effect, the shell radius depends very weakly on the ambient density, $R_{sh} \propto n_0^{-1/5}$, and H I densities do not vary by more than an a factor of 3 to 4 across the disk. It is unlikely, then, that shells in the outer

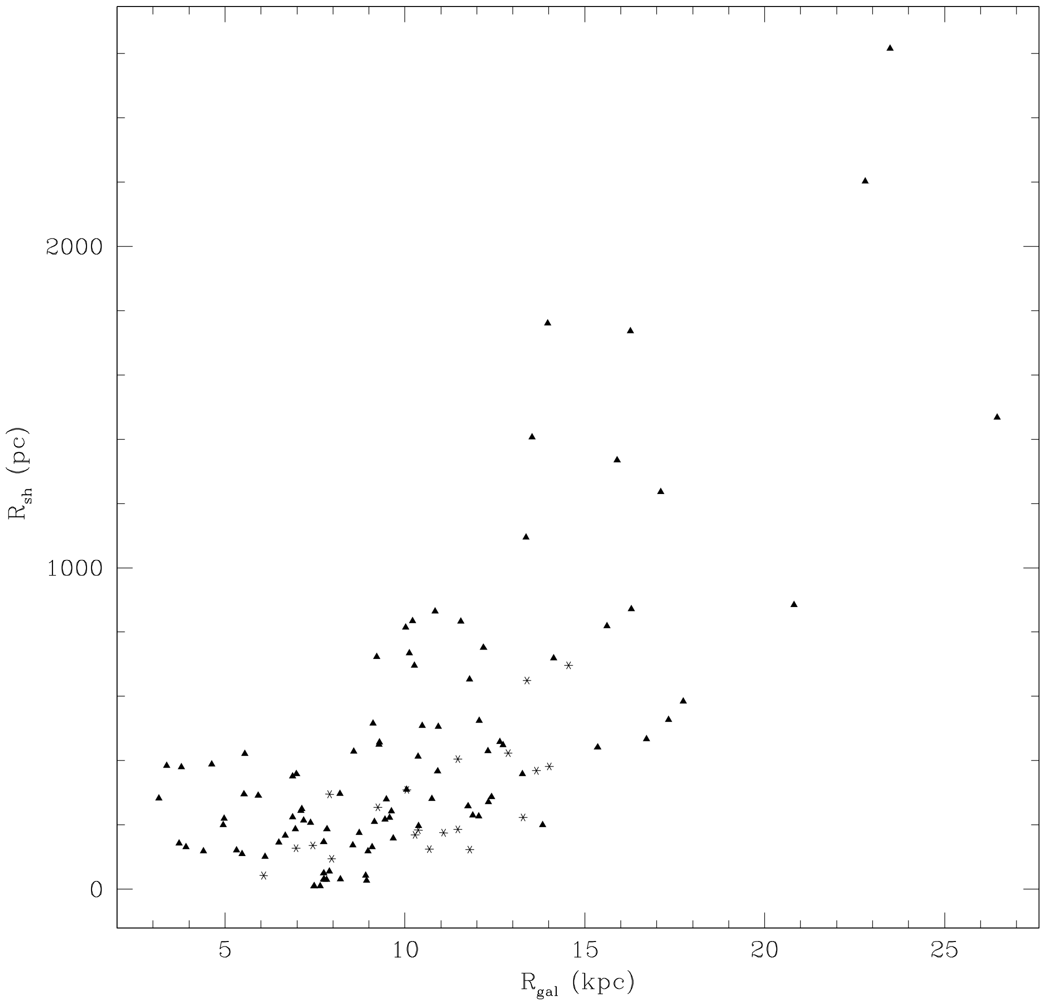


Figure 8.1: Galactic H I shell radius versus galactocentric radius. All shells from the SGPS are plotted with asterisks and shells from Heiles (1979, 1984) are plotted with triangles. The general trend that large shells are found at large galactocentric radii is clear.

Galaxy grow larger than those in the inner Galaxy by more than a factor of $\sim 1.3$ due to external density variation alone. This does not seem to be large enough of an effect to explain the distribution shown in Fig. 8.1.

Expansion energies also seem to be larger for shells in the outer Galaxy. Three out of the four most energetic shells from the SGPS are at $R_g > 10$ kpc. Calculated expansion energy is slightly more dependent than radius on the ambient density, $E_E \propto n_0^{1.12}$, and hence energetic shells may be partially explained by low ambient densities. In addition, Walter & Brinks (1999) point out that the constant in the expansion energy equation ($5.3 \times 10^{43}$ in equation 3.1) is dependent on cooling rates and includes an assumption about elemental abundances. Elemental abundances are not constant throughout the Galaxy, though, and are thought to decrease by more than an order of magnitude with Galactic radius (Shaver et al. 1983). Because metals are efficient at cooling, in a high metallicity environment more energy will be required for a shell to attain a given radius. Therefore, for shells in the outer Galaxy where the metallicities are lower, the expansion energies may be over-estimated.

Another avenue is to examine how H I shells are spatially related to Galactic spiral structure. Thilker (1999) found a strong correlation between spiral arms and H I shells in NGC 2403, M81 and M101. In these galaxies the shells are located along the spiral arms, usually extending into the interarm regions. Other galaxies also show shells between the spiral arms. Deul & den Hartog (1990) noted the presence of large H I holes in interarm regions of M33. NGC 4214 has three large shells between the spiral arms, and no detectable shells in the arms (McIntyre 2001; Walter et al. 2001). As mentioned in earlier chapters, some of the SGPS shells seem to extend into interarm regions; GSH 277+00+36 and GSH 280+00+59 are particularly clear examples. We would like, therefore, to compare all of our shells with the Milky Way spiral arms. Unfortunately, spiral structure in the Milky Way is poorly understood. Our unique position within the Galaxy makes tracing the spiral structure particularly difficult. The number of spiral arms, placement of the arms, and even the H I response of the spiral arms are all largely unknown. The main problem is the necessity of a well understood rotation curve to calculate kinematic distances. The Milky Way rotation curve is uncertain, as are the exact effects of streaming motions. Molecular line emission and H II regions are often used as tracers of spiral structure, but interpretations of these also rely on kinematic distances.

In order to eliminate the rotation curve dependence it is often preferable to address Galactic distributions with respect to the longitude-velocity ($l$-$v$) distribution, which does not include any assumptions about distance. In Fig. 8.2 we have plotted the SGPS shells on the $^{12}$CO $l$-$v$ diagram from Dame et al. (1987). The CO emission has been averaged for latitudes over the range $|b| < 2°$. Also included on this figure are H II regions from Caswell & Haynes (1987) marked with yellow crosses. The shells, marked by red ellipses, are located at their cataloged positions and their plotted sizes are determined by their angular diameters and velocity widths. Over the range $v = -100$ km s$^{-1}$ to $v = 0$ km s$^{-1}$ and $l > 310°$ the velocity structure is complicated and consequently the positions of the spiral arms are unclear. The only spiral arm that is immediately distinguished is part of the Sagittarius-Carina arm known as the "Carina Loop," marked with dashed lines on Fig. 8.2. The small chimney-like structure, GSH 298-01+32, is embedded in the edge of this spiral arm, apparently containing, or perhaps even a result of, an H II region. Outside of the loop, towards more positive velocities the shells GSH 277+00+36, GSH 280+00+59, GSH 292-01+55, and GSH 297-00+72 seem to follow the arc of the loop. Another noteworthy feature is the placement of GSH 304-00-12 (large ellipse at the center of Fig. 8.2) in an interarm region and bounded by CO emission from the Coalsack nebula near $v = 0$ km s$^{-1}$.

To expand the distribution study to more global scales, we have included the shells with $|b| < 5°$ from Heiles (1979, 1984). Figure 8.3 is a diagram of H I shells from the SGPS and Heiles (1979, 1984) plotted on the spiral arms of the Galaxy as defined in

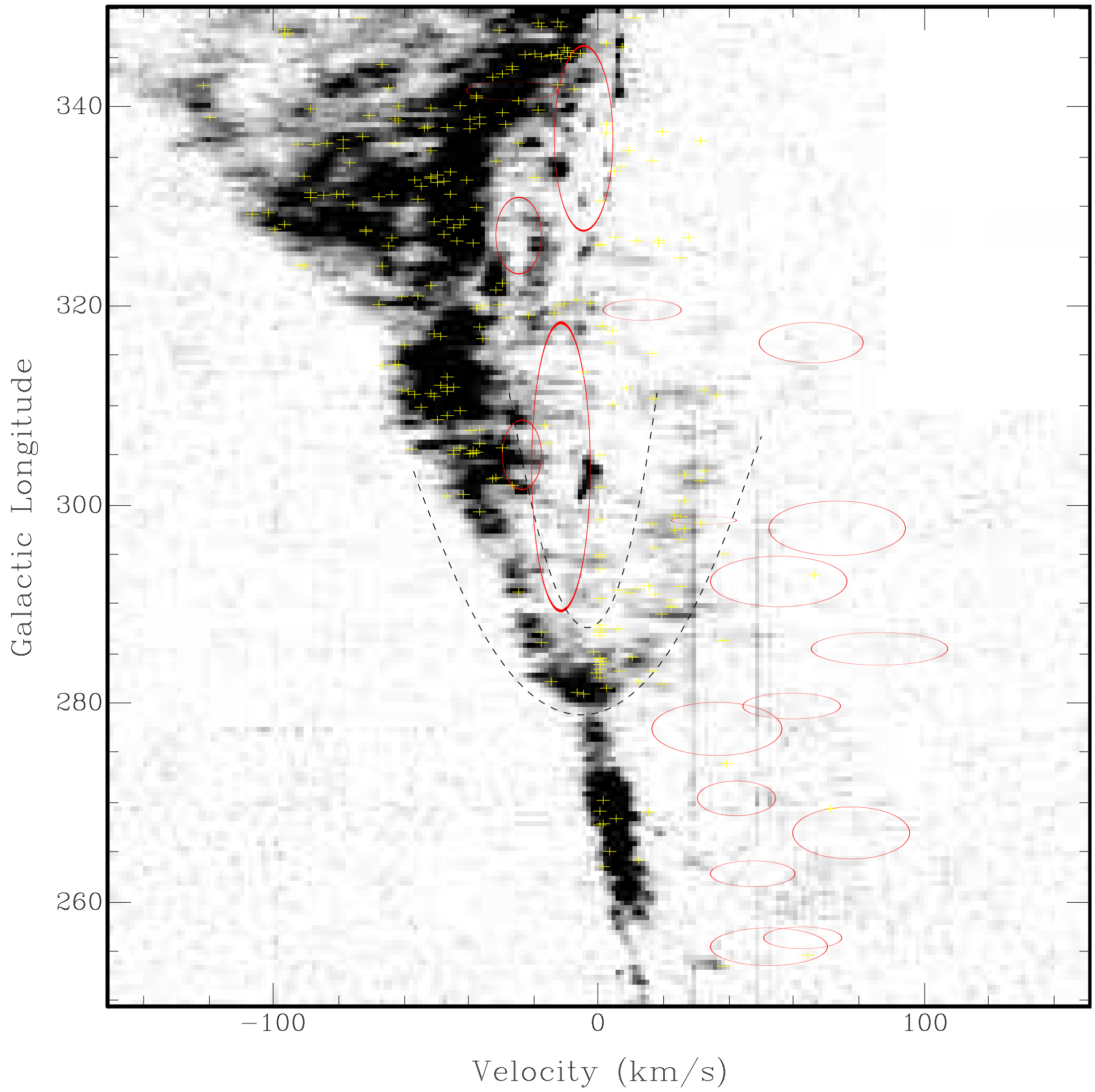


Figure 8.2: SGPS H I shells plotted on the $^{12}$CO $l$-$v$ image from Dame et al. (1987). The red ellipses mark the SGPS shells and the yellow crosses mark H II regions cataloged by Caswell & Haynes (1987) on the basis of their recombination lines. The dashed lines outline the "Carina Loop," part of the Sagittarius-Carina arm

the Taylor & Cordes (1993) electron density model. The Taylor & Cordes (1993) model fits the arms on the basis of the Georgelin & Georgelin (1976) spiral model from H II regions and radio-continuum features that mark the spiral arm tangents. The model is intended to describe the electron density distribution of the Galaxy, which is very much related to star formation, and it is, therefore, the most complete predictor of the spiral arm positions that we have. The arms given by Taylor & Cordes (1993) have been extended (narrow lines on Fig. 8.3) to approximate a spiral pattern. It should be stressed, though, that the extensions are extrapolations and are not based on spiral tracers. Shell positions are also uncertain; departures from circular rotation caused either by the underlying spiral pattern or other systemic effects are not accounted for in their positions. These departures can be as high as $\sim 10$ km s$^{-1}$, and therefore the positions of all shells are quite uncertain.

The Heiles (1979, 1984) shells are on the right-hand side of the figure and the shells to the left are from the SGPS. Many of the large cluster of local shells from the Heiles (1979, 1984) catalog seem to lie between the Sagittarius-Carina arm and the Perseus arm. Among the SGPS shells, some are clearly located between the spiral arms. The extreme distance of several of the shells, however, makes it difficult to compare them to the spiral arms because they are beyond the known extent of the arms.

Figs. 8.2 & 8.3 seem to suggest that an appreciable number of H I shells are located adjacent to spiral arms. Many shells also overlap spiral arms, so it is not a global trend. The most convincing examples of interarm shells are the outer Galaxy chimneys, GSH 277+0+36 and GSH 280+0+59, and the Coalsack shells, GSH 305+01-24 and GSH 304+00-12, which are all found on the edge of the Sagittarius-Carina spiral arm and open into the interarm region. However, because the *l*-*v* diagram only clearly shows one portion of a spiral arm, and the distribution of shells from a "bird's eye" view of the Galaxy is subject to distance determination uncertainties it is not possible to determine how common the correlation is. There are enough shells between spiral arms, though,

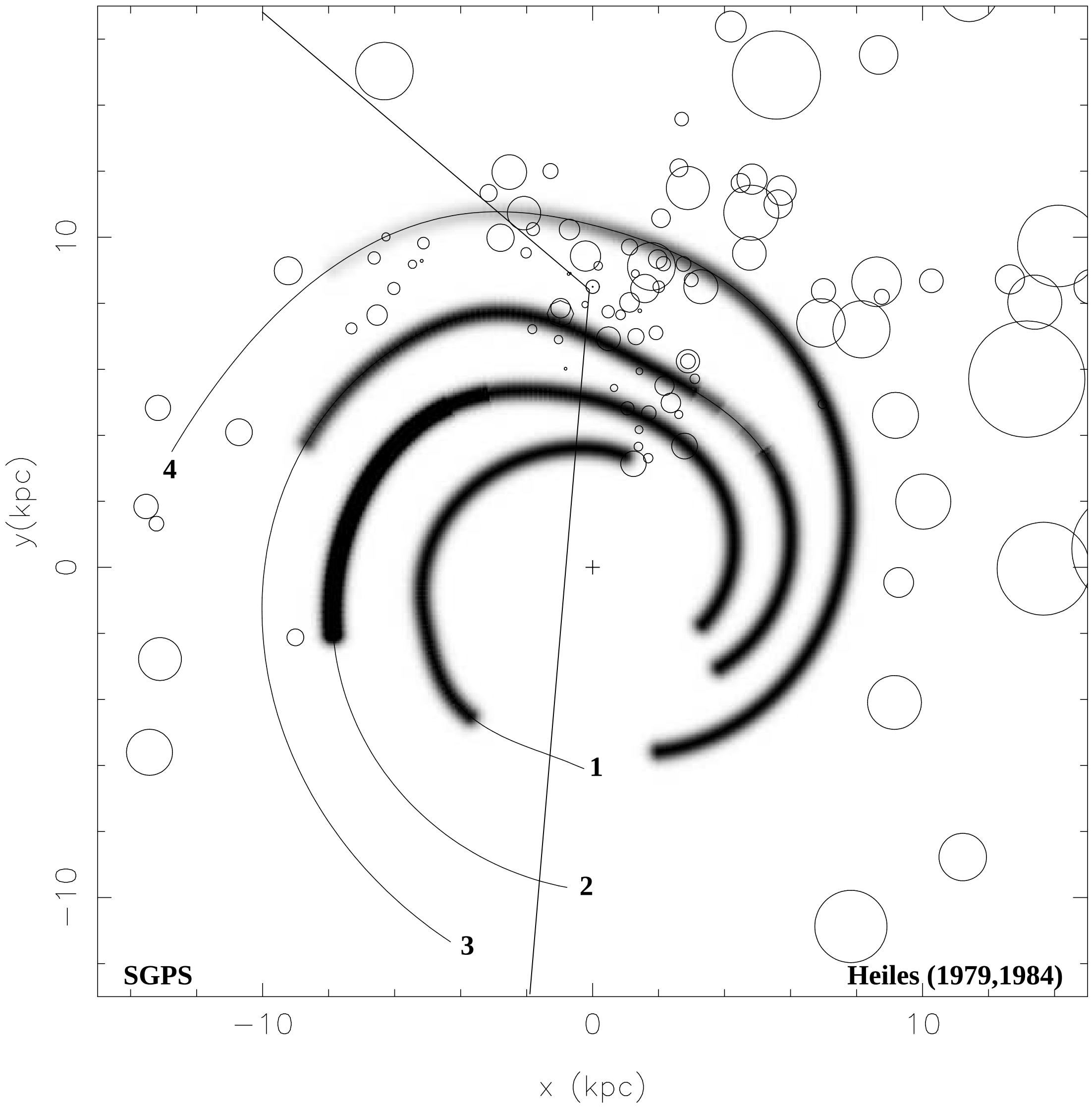


Figure 8.3: Cataloged shells plotted on the spiral pattern of the Galaxy from Taylor & Cordes (1993). As marked, shells in the first and second quadrant are from Heiles (1984) and shells in the fourth quadrant are from this work. The spiral arms are labeled 1-4 according to the following **1**: Norma, **2**: Scutum-Crux, **3**: Sagittarius-Carina, and **4**: Perseus. The Galactic center is marked by a cross-hair and the position of the Sun is marked by circle with a dot at the center.

to raise the question: why are they there?

## 8.3 Possible Causes for the Distribution

A priori one can think of several reasons that H I shells might be found between spiral arms and that large H I shells are found at large Galactic radii. First, star formation is concentrated downstream from a spiral shock. If the first wave of star formation occurs on the leading edge of the spiral arm then we might expect to see small H I shells formed from several stars located there. As the density wave passes through the disk, triggering more star formation, an H I shell can carve out a progressively larger and larger volume of the ISM. This is accompanied by the movement of the spiral arm such that by the time a large shell has been created, the gas will have moved away from the spiral arm. This argument can be supported by some very simple arguments about the timescales involved.

The frequency, in units of $\kappa$, the epicyclic frequency, with which a spiral density wave encounters matter in a differentially rotating disk is given by:

$$\nu^2 = \frac{n^2(\Omega_p - \Omega)^2}{\kappa^2}, \tag{8.1}$$

where $\Omega_p$ is the angular velocity of the spiral pattern and $\Omega$ is the angular velocity of the gas in the disk. From the shape of the spiral arms the spiral pattern speed is estimated to be in the range 11 km s$^{-1} \leq \Omega_p \leq 15$ km s$^{-1}$ (Bowers & Deeming 1984). At a galactocentric radius of $\sim 9$ kpc, the gas and pattern speed are matched (Amaral & Lèpine 1997). Interior to this co-rotation radius, $R_{CR}$, the arms move slower than the gas, resulting in a spiral shock on the counter-clockwise side of the arms, or the side towards the Galactic center. Star formation occurs near the spiral shock where gas compression due to the shock leads to molecular cloud condensation. Exterior to the co-rotation radius the arms move faster than the disk gas, and hence the spiral shock is on the exterior edge of the arms. At a galactic radius of 8 kpc, the spiral arms travel with a linear velocity, $v = \Omega_p R_{gal} \approx 120$ km s$^{-1}$. At the same distance, however, the gas in the disk rotates with a velocity of 220 km s$^{-1}$. Therefore, for an arm width of 3 kpc, the gas crosses the arm in $\sim 30$ Myr, which is comparable to the formation timescale for a large H I shell (Oey & Clarke 1997). By comparison, at a Galactic radius of 3 kpc, the arms only move at $\sim 45$ km s$^{-1}$, whereas the gas still travels at 220 km s$^{-1}$. In this case, the gas crosses a 3 kpc spiral arm in less than $\sim 17$ Myr, but more importantly, it also crosses the interarm region in a comparable amount of time. Therefore, a shell at a Galactic radius of $< 5$ kpc formed in a spiral arm will move out of the arm and encounter the next arm before it reaches its maximum radius. The encounter with the next spiral shock should be enough to completely disrupt the shell. It may be for this reason that large shells are only seen in the outer Galaxy, at small radii they do not survive long enough to reach a large size.

### 8.3.1 Simple Spiral Structure Model

Another important component to the shell distribution may be the density gradient in the transition from spiral arm to interarm region. Because the potential well at the back-side of the arm is not as steep as the front and there are no shocks, shells can escape and expand along the density gradient. To understand this gradient we need to understand the spiral perturbation in the disk.

We follow the arguments of Roberts & Hausman (1984) who define the two-dimensional, spirally perturbed disk gravitational potential as

$$U(r,\theta,t) = U_0(r)\left\{1 + \xi(r)\cos\left[m\theta - m\Omega_p t + \Phi(r)\right]\right\}, \tag{8.2}$$

where $r$ is the galactocentric radius, $\theta$ is the azimuthal angle, $U_0$ is the unperturbed potential, $\Omega_p$ is the pattern speed, and $\xi$ and $\Phi$ are the amplitude and phase, respectively, of the spiral perturbation. The unperturbed potential, $U_0$, is that of a Toomre disk (Toomre 1963) given by

$$U_0\,(r) = -\frac{B^2 a^3}{\left(a^2 + r^2\right)^{1/2}}, \tag{8.3}$$

where $a = 7$ kpc and $B = 0.0576$ Myr$^{-1}$ have been chosen in their model to give a peak circular velocity of 220 km s$^{-1}$ at 8.5 kpc. The amplitude of the spiral perturbation is,

$$\xi(r) = \frac{A}{5}\,\frac{a^2 r^2}{\left(a^2 + r^2\right)^2}. \tag{8.4}$$

The constant, $A = 0.067$, was chosen to make a spiral perturbing force that is $5 - 10\%$ of the unperturbed force. The phase of perturbation is given by

$$\Phi(r) = \frac{2\ln\left[1 + (r/r_0)^j\right]}{j\tan i_0}, \tag{8.5}$$

where $i_0$ is the pitch angle of the spiral, which is set to $10°$ here. The phase is defined to transition between a bar-like potential at $r < r_0 = 1$ kpc and a spiral-like potential at $r > r_0$. The power $j = 5$ determines how sharply this transition takes place.

We are concerned with the surface density response to the gravitational potential. We must therefore solve Poisson's equation for the surface density from the Toomre and spiral potentials. Given the unperturbed potential in equation 8.3, the unperturbed surface density from Roberts & Hausman (1984) is:

$$\sigma_o\,(r) = \frac{B^2 a^4}{2\pi G\left(a^2 + r^2\right)^{3/2}}. \tag{8.6}$$

Following Lin et al. (1969) and Freeman (1975) we solve Poisson's equation with the spiral potential for the linear density response of the total gas and stars by making an asymptotic approximation that the pitch angle is small and therefore the quantity $[\Phi'(r)r]^{-1}$ is small. The total surface density perturbation (gas and stars) is given by:

$$\sigma_p = \frac{U_o(r)\xi(r)}{2\pi G}\Phi'(r)\cos[m\theta - m\Omega_p t + \Phi(r)], \tag{8.7}$$

where $m$ is the number of arms. The total surface density, including the Toomre disk, is simply $\sigma_t = \sigma_o(r) + \sigma_p(r)$. Using the two-dimensional surface density given by these equations we modified the original Roberts & Hausman (1984) parameters to better fit the Georgelin & Georgelin (1976) and Taylor & Cordes (1993) model for the spiral arms. Rather than assuming a two-armed spiral we used a four-arm spiral with a pitch angle of $11\overset{\circ}{.}5$ and decreased the amplitude of the spiral perturbations so that $A = 0.05$. We found that these modifications gave a better fit to the Taylor & Cordes (1993) model for the spiral pattern.

The question of how the H I reacts to the spiral potential is non-trivial. The density derived in equation 8.7 neglects the effects of star formation, which through photo-dissociation may be significant in minimizing the arm-interarm density contrasts in H I. In addition, while the stellar disk dominates the mass density at small galactic radii, the gas disk dominates over the stellar disk for large radii. We have therefore modified the surface density to reflect the smaller arm-interarm contrasts seen in the Galaxy (Burton 1988) and to decrease the axisymmetric drop in density. We relate the surface density to the volume density at midplane according to $\Sigma_{HI} = \sqrt{2\pi}\sigma_z \rho_{HI}(0)$, where $\sigma_z = 120$ pc (Dickey & Lockman 1990). Finally, the parameters have been adjusted to give a fiducial density of $n_{HI} \approx 0.3$ cm$^{-3}$ at the position of the Sun. The surface density using this model and overlaid with the Taylor & Cordes (1993) spiral arms is shown in Figure 8.4.

### 8.3.2 Density Gradient Vector

As suggested above, the ambient medium has an effect on the radius and energetics of a supershell. It has been shown that a shell expanding out of the plane will experience exaggerated expansion along the density gradient to the halo (e.g. Mac Low & McCray 1988). Though magnetic fields in the plane can confine a shell for $\sim 20$ Myr (Tomisaka 1998), models show that the effect of the density gradient will be enough for a large shell to eventually blow out of the plane. Similarly, we wish to understand the density gradient around spiral arms in order to understand what effect the spiral arms and

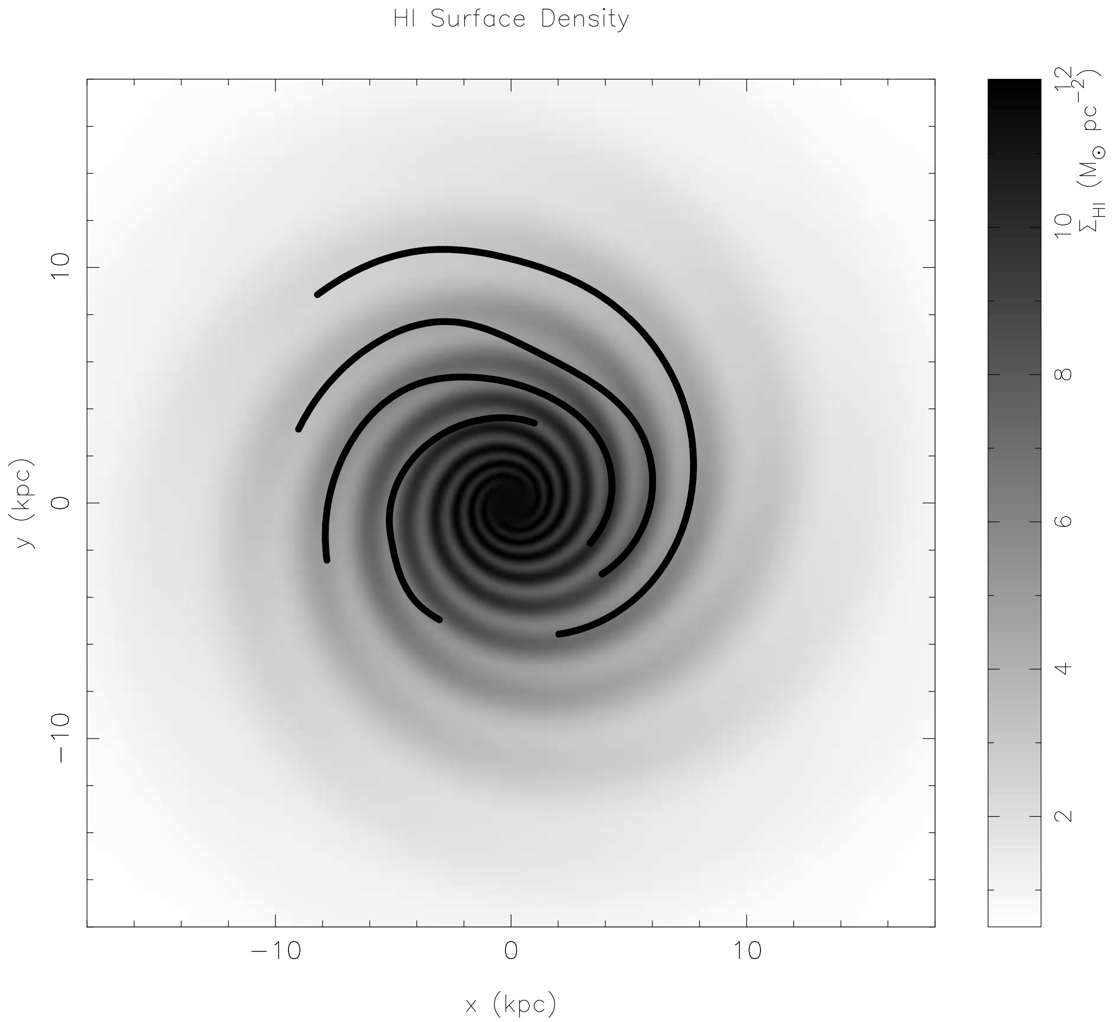


Figure 8.4: Greyscale image of the modeled H I surface density for the Galaxy as described by equations 8.2-8.7. The heavy lines trace the spiral arms as fit by Taylor & Cordes (1993). The greyscale ranges from 0 to 890 $M_\odot$ pc$^{-2}$. The pitch angle and number of arms have been modified from Roberts & Hausman (1984) to match the arms fit by Taylor & Cordes (1993).

interarm regions have on shells.

Figures 8.5 and 8.6 show radial and $z$ profiles of H I number density and density gradient. The radial profile was taken along the line-of-sight from the Sun to the Galactic center and the $z$ profile starts at mid-plane and extends to $z = 200$ pc. Obviously, both models grossly oversimplify the situation, but they are instructive to show how the density varies across the disk and out of the plane. Also shown in Fig. 8.5 is a density gradient calculated from just the spiral perturbation to the density, but not including the underlying axisymmetric disk. This should allow for a more direct comparison of the gradient in the plane and that out of the plane. Comparing the two models, we find that the density gradient 100 pc above the plane and the density gradient at the back edge of spiral arms are of comparable magnitude. Close to the Galactic plane an expanding shell will feel a pressure gradient away from the spiral arm that dominates that out of the plane. Consequently the shell should expand rapidly away from the arm. Towards the arm, expansion will be impeded by the high density medium. As the shell continues to expand vertically it will reach a $z$-height of $\sim 100$ pc, at which point the density gradient out of the plane should dominate.

This scenario is best understood when applied to GSH 277+00+36. In the early stages of its evolution the shell probably expanded away from the spiral arm into a region where the density was slightly less than at its central position. However, at about 100 pc, the gradient out of the plane began to dominate and the shell expanded quickly into the halo. The rapid expansion and pressure differential between the halo gas and the pressurized shell interior may have resulted in Rayleigh-Taylor instabilities that formed the chimney channels seen extending from the shell to the halo.

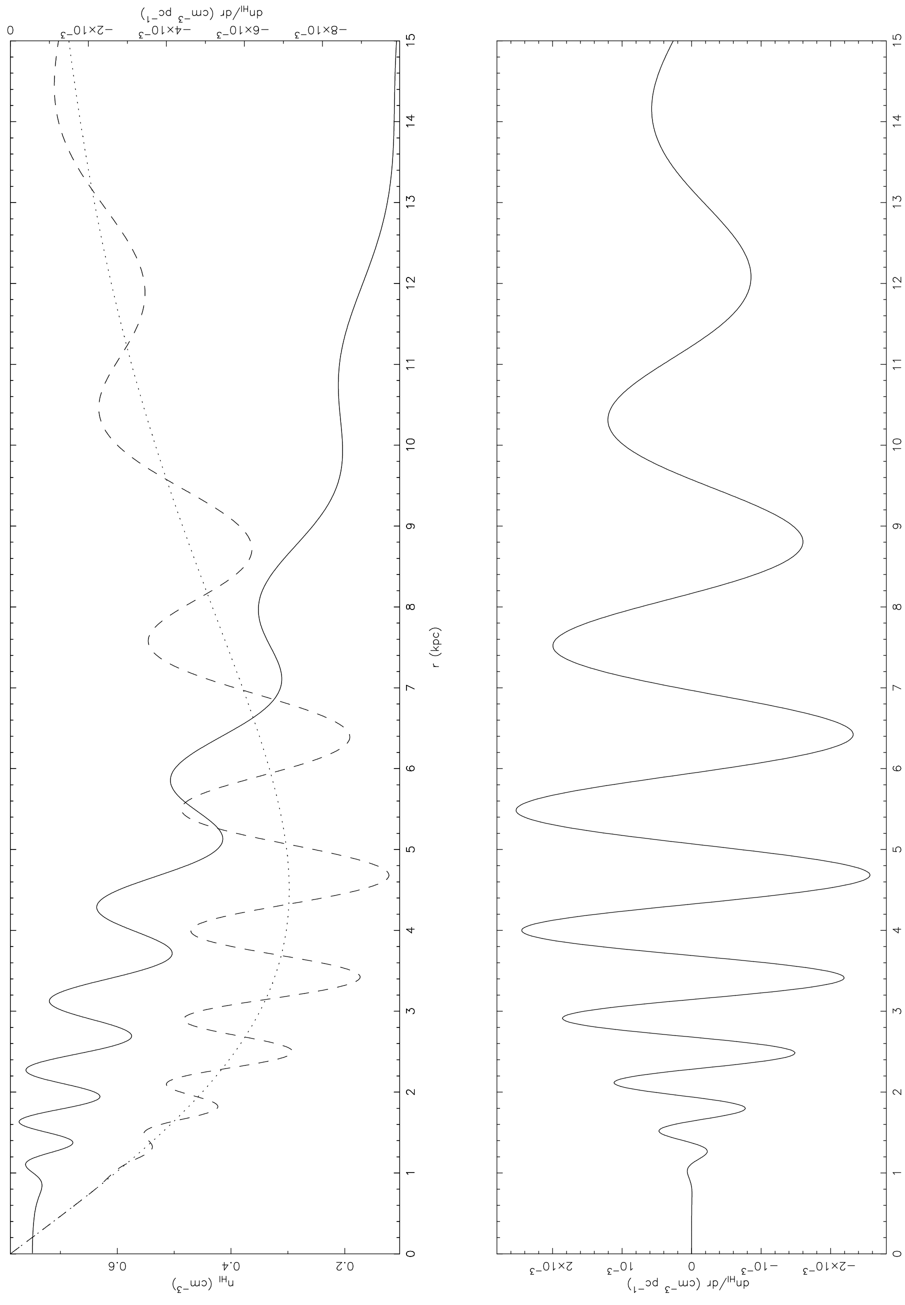


Figure 8.5: H I density and density gradient along the line of sight crossing the Sun and the Galactic center. The top panel shows the H I density profile, $n_{HI}(r)$, with a solid line. The dashed line is the one-dimensional density gradient profile, $dn_{HI}(r)/dr$, and the dotted line is density gradient for an axisymmetric potential, not including the spiral perturbation. The scale for the volume density is at the left and the scale for the density gradient is shown on the right. The bottom panel is the residual density gradient obtained by subtracting the axisymmetric component from the total density gradient. This plot shows the effect of the spiral arms alone.

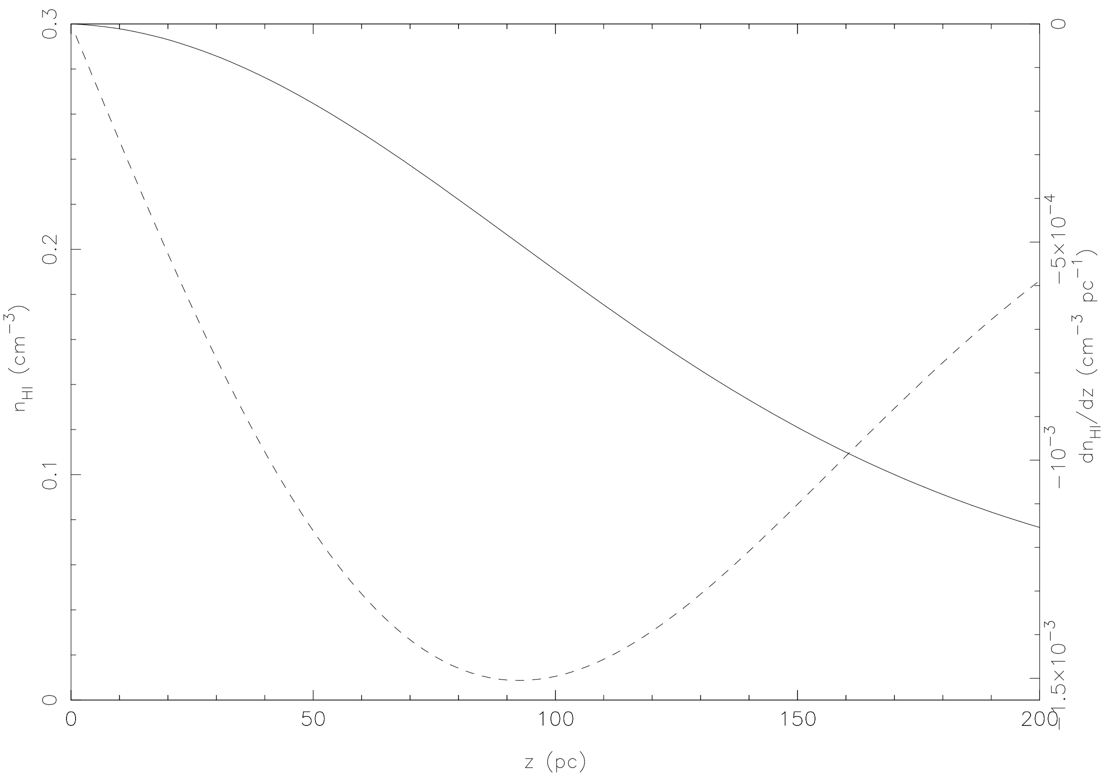


Figure 8.6: H I density and density gradient as a function of height above the galactic plane, $z$. The solid line is the H I number density with the axis marked to the left. The dashed line is the density gradient, $dn_{HI}/dz$, with the axis marked on the right.

## 8.4 Discussion

This model presents a possible explanation for the observation that many shells are between the spiral arms. A similar observation was made by Crosthwaite et al. (2000), who came to a different conclusion. Crosthwaite et al. (2000) examined the H I in the spiral galaxy IC 342 and found several large, shell-like structures in the outer galaxy ($R > R_{CR}$, where $R_{CR}$ is the co-rotation radius). In particular, they address the question of whether the fine structure in the spiral arms is due to shells or flocculent arms. They determine that the holes do not have the kinematic signatures of shells, that they are not necessarily associated with star formation in the form of H$\alpha$ emission or H II regions, that the energy requirements are too large, $E_E \sim 3 \times 10^{53}$ ergs, and most importantly, they argue that the shells do not appear to be experiencing shearing due to differential rotation. From this last point they argue that shearing would have significantly effected their observed shells in the timescales required to create holes that large with stellar winds and supernovae. They instead explore the possibilities that the structures were formed from negative shear that created spurs on the gas arms or alternately, that the flocculent structure is due to gas instabilities that created shell-like structures and holes, similar to the instabilities suggested by Wada & Norman (1999). They determine that the surface density enhancements in the spiral arm segments are insufficient to promote negative shear and hence perpendicular arm-spurs. They therefore conclude that the data supports they hypothesis that the shell-like structures are formed from two-fluid gravitational instabilities in the gas disk. Flocculent structure is seen in other spiral galaxies (e.g. Thornley & Mundy 1997, NGC5055), where there is indication for an underlying spiral structure, implying that flocculent spirals may be less developed forms of grand design spirals.

It is not impossible that many of the shells seen at the edges of arms in the Milky Way are also due to gravitational instabilities. However, in our limited sample of SGPS shells, the kinematic signatures are distinctly characteristic of expanding structures. Also, as argued in Chapter 5, the structure of the shell walls is characteristic of compression formed shells. GSH 277+0+36, for example, exhibits a very sharp shell wall and is cohesive over more than 40 km $s^{-1}$ of velocity dispersion. Both characteristics seem improbable for an object formed by gravitational instability. Perhaps, instead, the flocculent structure seen in the Milky Way is due to shells shredding the edges of spiral arms, rather than the suggestion of Crosthwaite et al. (2000).

## 8.5 Conclusions

We have examined the distribution of large H I shells in the Milky Way. We find a tendency for large, energetic shells to be located at large galactocentric radii. We also show that many shells are located between the spiral arms of the Galaxy. We have used spiral theory to show that the timescales are such that gas moves out of a spiral arm in about the time it takes to form a large ($R > 100$ pc) shell. We believe, then, that large shells will often be observed between the spiral arms. Additionally, we have used the same timescale arguments to show that in the inner Galaxy, where few large shells are observed, a shell would move out of an arm, through the interarm region, and be struck by the next spiral arm before it could reach an extremely large size. This may explain why large shells are only seen at large Galactic radii.

We have also used spiral theory to explore the radial density structure as a result of spiral arms. We compared this to the density structure extending out of the Galactic plane, towards the halo, and found that the density gradients are comparable. We know that shells expanding out of the plane tend to elongate in that direction and by analogy we suggest that a shell will expand away from a spiral arm in the same way. The shell would likely experience the same type of instabilities that lead to chimney formation. This may lead to large numbers of excessively large shells between the spiral arms. Clearly, further work is needed to explore these concepts.